Nuclear physics and core collapse supernovae

K. Langanke[1]

[1] *Institut for Fysik og Astronomi, Århus Universitet*
DK-8000 Århus C, Denmark

Nuclear physics plays an essential role in the dynamics of a collapsing massive stars, a type II supernova. Recent advances in nuclear many-body theory allow now to reliably calculate the stellar weak-interaction processes involving nuclei. The most important process is the electron capture on finite nuclei with mass numbers $A > 55$. It is found that the respective capture rates, derived from modern many-body models, differ noticeably from previous, more phenomenological estimates. This leads to significant changes in the stellar trajectory during the supernova explosion, as has been found in state-of-the-art supernova simulations.

The present article is based on a more detailed and extended manuscript appearing in Lecture Notes in Physics [1].

PACS numbers:

CORE COLLAPSE SUPERNOVAE - THE GENERAL PICTURE

At the end of hydrostatic burning, a massive star consists of concentric shells that are the remnants of its previous burning phases (hydrogen, helium, carbon, neon, oxygen, silicon). Iron is the final stage of nuclear fusion in hydrostatic burning, as the synthesis of any heavier element from lighter elements does not release energy; rather, energy must be used up. If the iron core, formed in the center of the massive star, exceeds the Chandrasekhar mass limit of about 1.44 solar masses, electron degeneracy pressure cannot longer stabilize the core and it collapses starting what is called a type II supernova. In its aftermath the star explodes and parts of the iron core and the outer shells are ejected into the Interstellar Medium. Although this general picture has been confirmed by the various observations from supernova SN1987a, simulations of the core collapse and the explosion are still far from being completely understood and robustly modelled. To improve the input which goes into the simulation of type II supernovae and to improve the models and their numerical simulations is a very active research field at various institutions worldwide.

The collapse is very sensitive to the entropy and to the number of leptons per baryon, Y_e [2]. In turn these two quantities are mainly determined by weak interaction processes, electron capture and β decay. First, in the early stage of the collapse Y_e is reduced as it is energetically favorable to capture electrons, which at the densities involved have Fermi energies of a few MeV, by (Fe-peak) nuclei. This reduces the electron pressure, thus accelerating the collapse, and shifts the distribution of nuclei present in the core to more neutron-rich material. Second, many of the nuclei present can also β decay. While this process is quite unimportant compared to electron capture for initial Y_e values around 0.5, it becomes increasingly competative for neutron-rich nuclei due to an increase in phase space related to larger Q_β values.

Electron capture, β decay and photodisintegration cost the core energy and reduce its electron density. As a consequence, the collapse is accelerated. An important change in the physics of the collapse occurs, as the density reaches $\rho_{\rm trap} \approx 4 \cdot 10^{11}$ g/cm^3. Then neutrinos are essentially trapped in the core, as their diffusion time (due to coherent elastic scattering on nuclei) becomes larger than the collapse time [3]. After neutrino trapping, the collapse proceeds homologously [4], until nuclear densities ($\rho_N > 10^{14}$ g/cm^3) are reached. As nuclear matter has a finite compressibility, the homologous core decelerates and bounces in response to the increased nuclear matter pressure; this eventually drives an outgoing shock wave into the outer core; i.e. the envelope of the iron core outside the homologous core, which in the meantime has continued to fall inwards at supersonic speed. The core bounce with the formation of a shock wave is believed to be the mechanism that triggers a supernova explosion, but several ingredients of this physically appealing picture and the actual mechanism of a supernova explosion are still uncertain and controversial. The energy available to the shock is not sufficient to stop the collapse and to explode the outer burning shells of the star. Rather the shock will store its energy in the outer core, for example, by dissociation of nuclei into nucleons. Furthermore, this change in composition results to additional energy losses, as the electron capture rate on free protons is significantly larger than on neutron-rich nuclei due to the smaller Q-values involved. This leads to a further neutronization of the matter. Part of the neutrinos produced by the capture on the free protons behind the shock leave the star carrying away energy.

After the core bounce, a compact remnant is left behind. Depending on the stellar mass, this is either a neutron star or a black hole. The neutron star remnant is very lepton-rich (electrons and neutrinos), the latter being trapped as their mean free paths in the dense matter is significantly shorter than the radius of the neutron star. It takes a fraction of a second [6] for the trapped neutrinos to diffuse out, giving most of their energy to the neutron star during that process and heating it up. The cooling of the protoneutron star then proceeds by pair production of neutrinos of all three generations which diffuse out. After several tens of seconds the star becomes transparent to neutrinos and the neutrino luminosity drops significantly [8].

In the 'delayed mechanism' [5], the shock wave can be revived by the outward diffusing neutrinos, which carry most of the energy set free in the gravitational collapse of the core [6] and deposit some of this energy in the layers between the nascent neutron star and the stalled prompt shock. This lasts for a few 100 ms, and requires about 1% of the neutrino energy to be converted into nuclear kinetic energy. The energy deposition increases the pressure behing the shock and the respective layers begin to expand, leaving between shock front and neutron star surface a region of low density, but rather high temperature. The persistent energy input by neutrinos keeps the pressure high in this region and drives the shock outwards again, eventually leading to a supernova explosion.

It has been found that the delayed supernova mechanism is quite sensitive to physics details deciding about success or failure in the simulation of the explosion. Very recently, two quite distinct improvements have been proposed (convective energy transport [9, 10] and in-medium modifications of the neutrino opacities [11, 12]) which increase the efficiency of the energy transport to the stalled shock.

Current one-dimensional supernova simulations, including sophisticated neutrino transport, fail to explode [7, 13] (however, see [14]). This is also true for very recent two-dimensional simulations [15]. The interesting question is whether the simulations explicitly requires multi-dimensional effects like rotation, magnetic fields or convection (e.g. [9, 10]) or whether the microphysics input in the one-dimensional models is insufficient. It is the goal of nuclear astrophysics to improve on this microphysics input. The next section shows that core collapse supernovae are nice examples to demonstrate how important micro-physics input and progress in nuclear modelling can be.

STELLAR ELECTRON CAPTURE AND β DECAY

Late-stage stellar evolution is described in two steps. In the presupernova models the evolution is studied through the various hydrostatic core and shell burning phases until the central core density reaches values up to 10^{10} g/cm^3. The models consider a large nuclear reaction network. However, the densities involved are small enough to treat neutrinos solely as an energy loss source. For even higher densities this is no longer true as neutrino-matter interactions become increasingly important. In modern core-collapse codes neutrino transport is described self-consistently by spherically symmetric multigroup Boltzmann simulations [7, 13, 15]. While this is computationally very challenging, collapse models have the advantage that the matter composition can be derived from Nuclear Statistical Equilibrium (NSE) as the core temperature and density are high enough to keep reactions mediated by the strong and electromagnetic interactions in equilibrium. This means that for sufficiently low entropies, the matter composition is dominated by the nuclei with the highest Q-values for a given Y_e. The presupernova models are the input for the collapse simulations which follow the evolution through trapping, bounce and hopefully explosion.

The collapse is a competition of the two weakest forces in nature: gravity versus weak interaction, where electron captures on nuclei and protons and, during a period of silicon burning, also β-decay play the crucial roles. Which nuclei are important? Weak-interaction processes become important when nuclei with masses $A \sim 55-60$ (pf-shell nuclei) are most abundant in the core (although capture on sd shell nuclei has to be considered as well). As weak interactions changes Y_e and electron capture dominates, the Y_e value is successively reduced from its initial value ~ 0.5. As a consequence, the abundant nuclei become more neutron-rich and heavier, as nuclei with decreasing Z/A ratios are more bound in heavier nuclei. Two further general remarks are useful. There are many nuclei with appreciable abundances in the cores of massive stars during their final evolution. Neither the nucleus with the largest capture rate nor the most abundant one are necessarily the most relevant for the dynamical evolution: What makes a nucleus relevant is the product of rate times abundance.

For densities $\rho \lesssim 10^{11}$ g/cm^3, stellar weak-interaction processes are dominated by Gamow-Teller (GT) and, if applicable, by Fermi transitions. At higher densities forbidden transitions have to be included as well. To understand the requirements for the nuclear models to describe these processes (mainly electron capture), it is quite useful to recognize that electron capture is governed by two energy scales: the electron chemical potential μ_e, which grows like $\rho^{1/3}$, and the nuclear Q-value. Further, μ_e grows much faster than the Q values of the abundant nuclei. We can conclude that at low densities, where one has $\mu_e \sim Q$ (i.e. at presupernova conditions), the capture rates will be very sensitive to the phase space and require an accurate as possible description of the detailed GT_+ distribution of the nuclei involved. Furthermore, the finite temperature in the star requires the implicit consideration of capture on excited nuclear states, for which the GT distribution can be different than for the ground state. As we will demonstrate below, modern shell model calculations are capable to describe GT_+ distributions rather well and are therefore the appropriate tool to calculate the weak-interaction rates for those nuclei ($A \sim 50-65$) which are relevant at such densities. At higher densities, when μ_e is sufficiently larger than the respective nuclear Q values, the capture rate becomes less sensitive to the detailed GT_+ distribution and is mainly only dependent on the total GT strength. Thus, less sophisticated nuclear models might be sufficient. However, one is facing a nuclear structure problem which has been overcome only very recently. We come back to it below, after we have discussed the calculations of weak-interaction rates within the shell model and their implications to presupernova models.

Weak-interaction rates and presupernova evolution

The general formalism to calculate weak interaction rates for stellar environment has been given by Fuller, Fowler and Newman (FFN) [16–19]. These authors also estimated the stellar electron capture and beta-decay rates systematically for nuclei in the mass range $A = 20-60$ based on the independent particle model and on data, whenever available. In recent years this pioneering and seminal work has been replaced by rates based on large-scale shell model calculations. At first, Oda *et al.* derived such rates for *sd*-shell nuclei ($A = 17-39$) and found rather good agreement with the FFN rates [20]. Similar calculations for pf-shell nuclei had to wait until significant progress in shell model diagonalization, mainly due to Etienne Caurier, allowed calculations in either the full pf shell or at such a truncation level that the GT distributions were virtually converged. It has been demonstrated in [21] that the shell model reproduces all measured GT_+ distributions very well and gives a very reasonable account of the experimentally known GT_- distributions. Further, the lifetimes of the nuclei and the spectroscopy at low energies is simultaneously also described well. Charge-exchange measurements using the (d,^{2}He) reaction at intermediate energies allow now for an experimental determination of the GT_+ strength distribution with an energy resolution of about 150 keV. Experimental GT_+ strengths, measured for several pf shell nuclei at the KVI in Groningen [23], agree well with shell model predictions. It can be concluded that modern shell model approaches have the necessary predictive power to reliably estimate stellar weak interaction rates. Such rates have been presented in [22, 25]. for more than 100 nuclei in the mass range $A =$ 45-65. The rates have been calculated for the same temperature and density grid as the standard FFN compilations [17, 18]. An electronic table of the rates is available [25]. Importantly one finds that the shell model electron capture rates are systematically smaller than the FFN rates.

To study the influence of the shell model rates on presupernova models Heger *et al.* [26, 27] have repeated the calculations of Weaver and Woosley [28] keeping the stellar physics, except for the weak rates, as close to the original studies as possible. Fig. 1 examplifies the consequences of the shell model weak interaction rates for presupernova models in terms of the three decisive quantities: the central Y_e value and entropy and the iron core mass. The central values of Y_e at the onset of core collapse increased by 0.01-0.015 for the new rates. This is a significant effect. We note that the new models also result in lower core entropies for stars with $M \leq 20M_\odot$, while for $M \geq 20M_\odot$, the new models actually have a slightly larger entropy. The iron core masses are generally smaller in the new models where the effect is larger for more massive stars ($M \geq 20M_\odot$), while for the most common supernovae ($M \leq 20M_\odot$) the reduction is by about 0.05 $M_\odot$.

Electron capture dominates the weak-interaction processes during presupernova evolution. However, during silicon burning, β decay (which increases Y_e) can compete and adds to the further cooling of the star. With increasing densities, β-decays are hindered as the increasing Fermi energy of the electrons blocks the available phase space for the decay. Thus, during collapse β-decays can be neglected.

We note that the shell model weak interaction rates predict the presupernova evolution to proceed along a temperature-density-Y_e trajectory where the weak processes are dominated by nuclei rather close to stability. Thus it will be possible, after radioactive ion-beam facilities become operational, to further constrain the shell model calculations by measuring relevant beta decays and GT distributions for unstable nuclei. Ref. [26, 27] identify those nuclei which dominate (defined by the product of abundance times rate) the electron capture and beta decay during various stages of the final evolution of a $15M_\odot$, $25M_\odot$ and $40M_\odot$ star.

The role of electron capture during collapse

In collapse simulations a very simple description for electron capture on nuclei has been used until recently, as the rates have been estimated in the spirit of the independent particle model (IPM), assuming pure Gamow-Teller (GT) transitions and considering only single particle states for proton and neutron numbers between $N =$ 20–40 [29]. In particular this model assigns vanishing electron capture rates to nuclei with neutron numbers larger than $N = 40$,

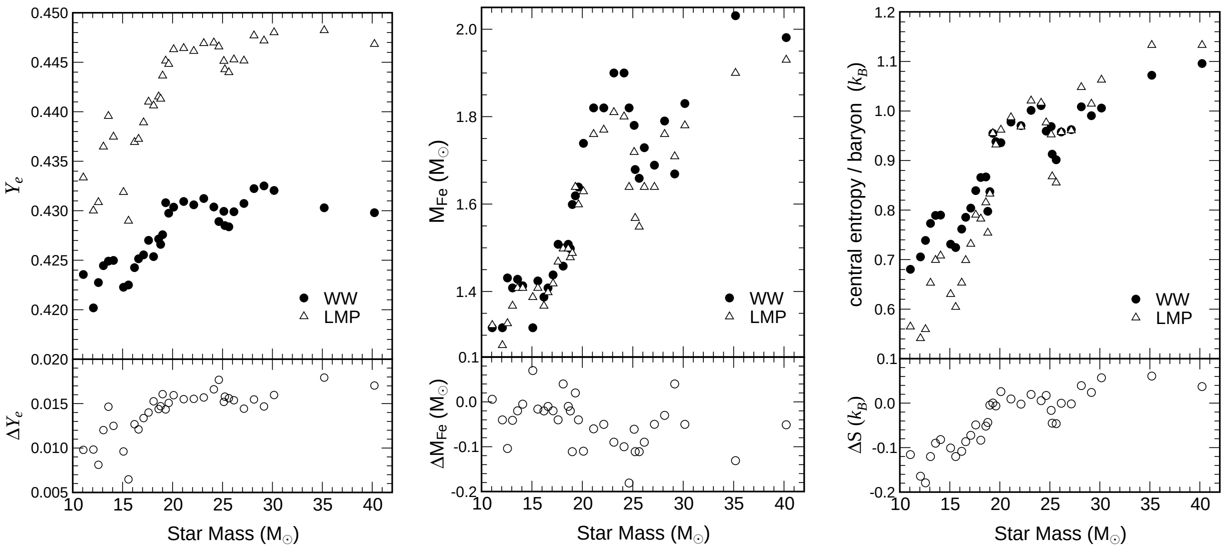

FIG. 1: Comparison of the center values of Y_e (left), the iron core sizes (middle) and the central entropy (right) for $11-40M_\odot$ stars between the WW models, which used the FFN rates, and the ones using the shell model weak interaction rates (LMP).

motivated by the observation [30] that, within the IPM, GT transitions are Pauli-blocked for nuclei with $N \geq 40$ and $Z \leq 40$. However, as electron capture reduces Y_e, the nuclear composition is shifted to more neutron rich and to heavier nuclei, including those with $N > 40$, which dominate the matter composition for densities larger than a few 10^{10} g cm^{-3}. As a consequence of the model applied in the previous collapse simulations, electron capture on nuclei ceases at these densities and the capture is entirely due to free protons. This employed model for electron capture on nuclei is too simple and leads to incorrect conclusions, as the Pauli-blocking of the GT transitions is overcome by correlations [32] and temperature effects [30, 31].

At first, the residual nuclear interaction, beyond the IPM, mixes the pf shell with the levels of the sdg shell, in particular with the lowest orbital, $g_{9/2}$. This makes the closed $g_{9/2}$ orbit a magic number in stable nuclei ($N = 50$) and introduces, for example, a very strong deformation in the $N = Z = 40$ nucleus ^{80}Zr [33]. Moreover, the description of the B(E2,$0^+ \rightarrow 2_1^+$) transition in ^{68}Ni requires configurations where more than one neutron is promoted from the pf shell into the $g_{9/2}$ orbit [34], unblocking the GT transition even in this proton-magic $N = 40$ nucleus. Such a non-vanishing GT strength has already been observed for ^{72}Ge ($N = 40$) [35] and ^{76}Se ($N = 42$) [36]. Secondly, during core collapse electron capture on the nuclei of interest here occurs at temperatures $T \gtrsim 0.8$ MeV, which, in the Fermi gas model, corresponds to a nuclear excitation energy $U \approx AT^2/8 \gtrsim 5$ MeV; this energy is noticeably larger than the splitting of the pf and sdg orbitals ($E_{g_{9/2}} - E_{p_{1/2},f_{5/2}} \approx 3$ MeV). Hence, the configuration mixing of sdg and pf orbitals will be rather strong in those excited nuclear states of relevance for stellar electron capture. Furthermore, the nuclear state density at $E \sim 5$ MeV is already larger than 100/MeV, making a state-by-state calculation of the rates impossible, but also emphasizing the need for a nuclear model which describes the correlation energy scale at the relevant temperatures appropriately. This model is the Shell Model Monte Carlo (SMMC) approach [37, 38] which describes the nucleus by a canonical ensemble at finite temperature and employs a Hubbard-Stratonovich linearization [39] of the imaginary-time many-body propagator to express observables as path integrals of one-body propagators in fluctuating auxiliary fields [37, 38]. Since Monte Carlo techniques avoid an explicit enumeration of the many-body states, they can be used in model spaces far larger than those accessible to conventional methods. The Monte Carlo results are in principle exact and are in practice subject only to controllable sampling and discretization errors.

To calculate electron capture rates for nuclei $A = 65$–112 SMMC calculations have been performed in the full pf-sdg shell, using a residual pairing+quadrupole interaction, which, in this model space, reproduces well the collectivity around the $N = Z = 40$ region and the observed low-lying spectra in nuclei like ^{64}Ni and ^{64}Ge. From the SMMC calculations the temperature-dependent occupation numbers of the various single-particle orbitals have been determined. These occupation numbers then became the input in RPA calculations of the capture rate, considering allowed and forbidden transitions up to multipoles $J = 4$ and including the momentum dependence of the operators. The method has been validated against capture rates calculated from diagonalization shell model studies for ^{64,66}Ni. The model is described in [32]; first applications in collapse simulations are presented in [41, 42].

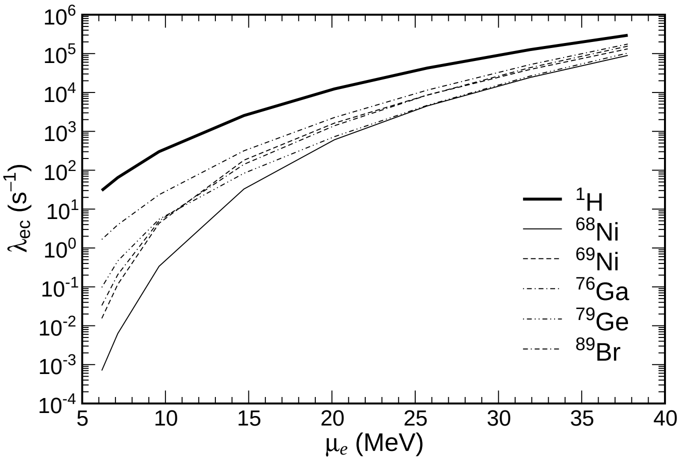

FIG. 2: Comparison of the electron capture rates on free protons and selected nuclei as function of the electron chemical potential along a stellar collapse trajectory taken from [7]. Neutrino blocking of the phase space is not included in the calculation of the rates.

For all studied nuclei one finds neutron holes in the (pf) shell and, for $Z > 30$, non-negligible proton occupation numbers for the *sdg* orbitals. This unblocks the GT transitions and leads to sizable electron capture rates. Fig. 2 compares the electron capture rates for free protons and selected nuclei along a core collapse trajectory, as taken from [7]. Dependent on their proton-to-nucleon ratio Y_e and their Q-values, these nuclei are abundant at different stages of the collapse. For all nuclei, the rates are dominated by GT transitions at low densities, while forbidden transitions contribute sizably at $\rho_{11} \gtrsim 1$.

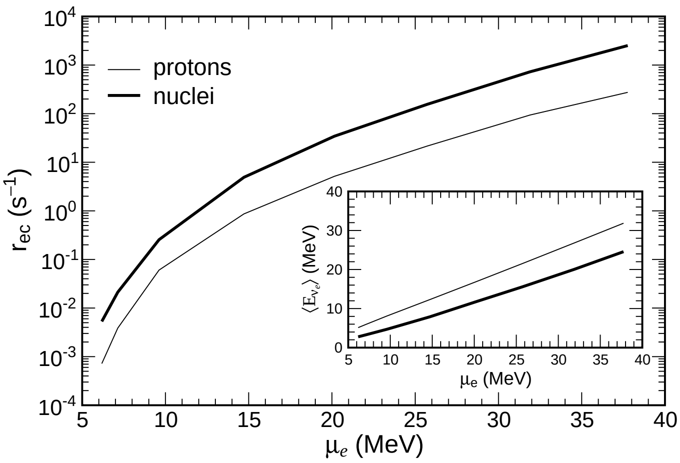

FIG. 3: The reaction rates for electron capture on protons (thin line) and nuclei (thick line) are compared as a function of electron chemical potential along a stellar collapse trajectory. The insert shows the related average energy of the neutrinos emitted by capture on nuclei and protons. The results for nuclei are averaged over the full nuclear composition (see text). Neutrino blocking of the phase space is not included in the calculation of the rates.

Simulations of core collapse require reaction rates for electron capture on protons, $R_p = Y_p \lambda_p$, and nuclei $R_h = \sum_i Y_i \lambda_i$ (where the sum runs over all the nuclei present and Y_i denotes the number abundance of a given species), over wide ranges in density and temperature. While R_p is readily derived from [29], the calculation of R_h requires knowledge of the nuclear composition, in addition to the electron capture rates described earlier. In [41, 42] a Saha-like NSE has been adopted to determine the needed abundances of individual isotopes and to calculate R_h and the associated emitted neutrino spectra on the basis of about 200 nuclei in the mass range $A = 45 - 112$ as a function of temperature, density and electron fraction. The rates for the inverse neutrino-absorption process are determined from the electron capture rates by detailed balance. Due to its much smaller $|Q|$-value, the electron capture rate on the free protons is larger than the rates of abundant nuclei during the core collapse (fig. 2). However, this is misleading as the low entropy keeps the protons significantly less abundant than heavy nuclei during the collapse. Fig. 3 shows that the reaction rate on nuclei, R_h, dominates the one on protons, R_p, by roughly an order of magnitude throughout the collapse when the composition is considered. (We note that this figure is based on a stellar trajectory which does not consider capture on nuclei. We will see below that this process dominates and reduces Y_e even more. As a consequence the abundance of free protons in NSE is significantly reduced, making capture on free protons even less important.) Only after the bounce shock has formed does R_p become higher than R_h, due to the high entropies and high temperatures in the shock-heated matter that result in a high proton abundance. The obvious conclusion is that electron capture on nuclei must be included in collapse simulations.

It is also important to stress that electron capture on nuclei and on free protons differ quite noticeably in the neutrino spectra they generate. This is demonstrated in Fig. 3 which shows that neutrinos from captures on nuclei have a mean energy 40–60% less than those produced by capture on protons. Although capture on nuclei under stellar conditions involves excited states in the parent and daughter nuclei, it is mainly the larger $|Q|$-value which significantly shifts the energies of the emitted neutrinos to smaller values. These differences in the neutrino spectra strongly influence neutrino-matter interactions, which scale with the square of the neutrino energy and are essential for collapse simulations [7, 13] (see below).

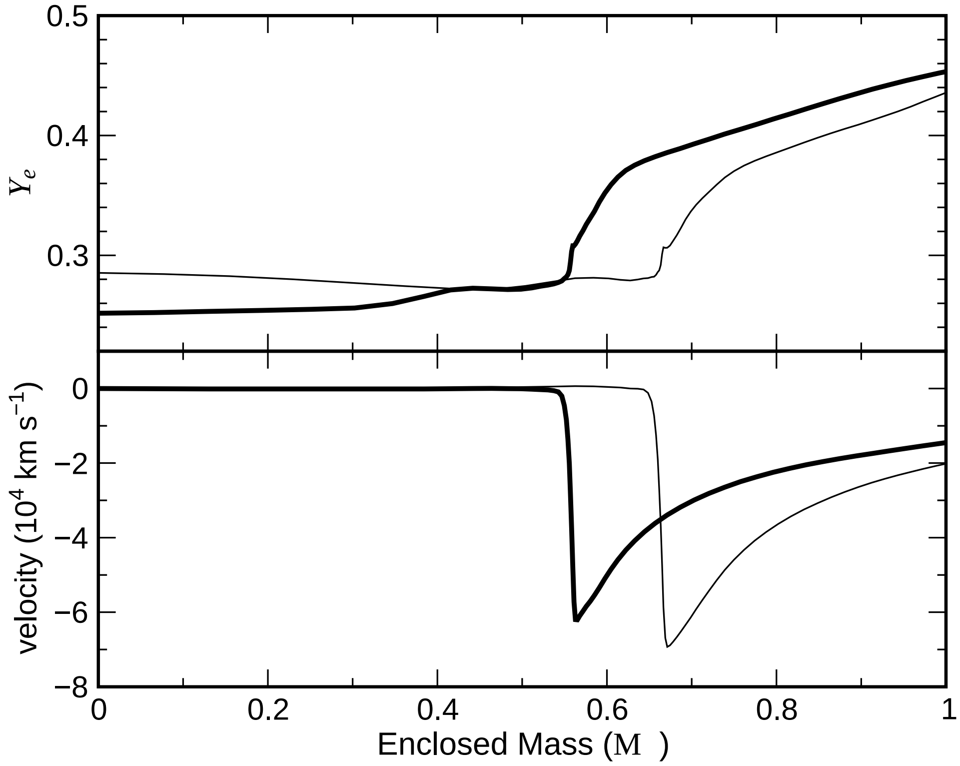

FIG. 4: The electron fraction and velocity as functions of the enclosed mass at bounce for a 15 $M_\odot$ model [26]. The thin line is a simulation using the Bruenn parameterization while the thick line is for a simulation using the combined LMP [22] and SMMC+RPA rate sets.

The effects of this more realistic implementation of electron capture on heavy nuclei have been evaluated in independent self-consistent neutrino radiation hydrodynamics simulations by the Oak Ridge and Garching collaborations [42, 43]. The basis of these models is described in detail in Refs. [7] and [13]. Both collapse simulations yield qualitatively the same results. The changes compared to the previous simulations, which adopted the IPM rate estimate from Ref. [29] and hence basically ignored electron capturei on nuclei, are significant. Fig. 4 shows a key result: In denser regions, the additional electron capture on heavy nuclei results in more electron capture in the new models. In lower density regions, where nuclei with $A < 65$ dominate, the shell model rates [22] result in less electron capture. The results of these competing effects can be seen in the first panel of Figure 4, which shows the distribution of Y_e throughout the core at bounce (when the maximum central density is reached). The combination of increased electron capture in the interior with reduced electron capture in the outer regions causes the shock to form with 16% less mass interior to it and a 10% smaller velocity difference across the shock. This leads to a smaller mass of the homologuous core (by about 0.1 $M_{\odot}$). In spite of this mass reduction, the radius from which the shock is launched is actually displaced slightly outwards to 15.7 km from 14.8 km in the old models. If the only effect of the improvement in the treatment of electron capture on nuclei were to launch a weaker shock with more of the iron core overlying it, this improvement would seem to make a successful explosion more difficult. However, the altered gradients in density and lepton fraction also play an important role in the behavior of the shock. Though also the new models fail to produce explosions in the spherically symmetric limit, the altered gradients allow the shock in the case with improved capture rates to reach 205 km, which is about 10 km further out than in the old models.

These calculations clearly show that the many neutron-rich nuclei which dominate the nuclear composition throughout the collapse of a massive star also dominate the rate of electron capture. Astrophysics simulations have demonstrated that these rates have a strong impact on the core collapse trajectory and the properties of the core at bounce. The evaluation of the rates has to rely on theory as a direct experimental determination of the rates for the relevant stellar conditions (i.e. rather high temperatures) is currently impossible. Nevertheless it is important to experimentally explore the configuration mixing between pf and sdg shell in extremely neutron-rich nuclei as such understanding will guide and severely constrain nuclear models. Such guidance is expected from future radioactive ion-beam facilities.

NEUTRINO-INDUCED PROCESSES DURING A SUPERNOVA COLLAPSE

While the neutrinos can leave the star unhindered during the presupernova evolution, neutrino-induced reactions become more and more important during the subsequent collapse stage due to the increasing matter density and neutrino energies; the latter are of order a few MeV in the presupernova models, but increase roughly approximately to the electron chemical potential [29, 32]. Elastic neutrino scattering off nuclei and inelastic scattering on electrons are the two most important neutrino-induced reactions during the collapse. The first reaction randomizes the neutrino paths out of the core and, at densities of a few 10^{11} g/cm^3, the neutrino diffusion time-scale gets larger than the collapse time; the neutrinos are trapped in the core for the rest of the contraction. Inelastic scattering off electrons thermalizes the trapped neutrinos then rather fastly with the matter.

Neutrino-induced reactions on nuclei, other than elastic scattering, can also play a role during the collapse and explosion phase [44]. Note that during the collapse only ν_e neutrinos are present. Thus, charged-current reactions $A(\nu_e, e^-)A'$ are strongly blocked by the large electron chemical potential [45, 46]. Inelastic neutrino scattering on nuclei can compete with $\nu_e + e^-$ scattering at higher neutrino energies $E_\nu \geq 20$ MeV [45]. Here the cross sections are mainly dominated by first-forbidden transitions. Finite-temperature effects play an important role for inelastic $\nu + A$ scattering below $E_\nu \leq 10$ MeV. This comes about as nuclear states get thermally excited which are connected to the ground state and low-lying excited states by modestly strong GT transitions and increased phase space. As a consequence the cross sections are significantly increased for low neutrino energies at finite temperature and might be comparable to inelastic $\nu_e + e^-$ scattering [47]. Thus, inelastic neutrino-nucleus scattering, which is so far neglected in collapse simulations, should be implemented in such studies. This is in particular motivated by the fact that it has been demonstrated that electron capture on nuclei dominated during the collapse and this mode generates significantly less energetic neutrinos than considered previously. Examples for inelastic neutrino-nucleus cross sections are shown in Fig. 5. A reliable estimate for these cross sections requires the knowledge of the GT$_0$ strength. Shell model predictions imply that the GT$_0$ centroid resides at excitation energies around 10 MeV and is independent of the pairing structure of the ground state [47, 48]. Finite temperature effects become unimportant for stellar inelastic neutrino-nucleus cross sections once the neutrino energy is large enough to reach the GT_0 centroid, i.e. for $E_\nu \geq 10$ MeV.

The trapped ν_e neutrinos will be released from the core in a brief burst shortly after bounce. These neutrinos can interact with the infalling matter just before arrival of the shock and eventually preheat the matter requiring less energy from the shock for dissociation [44]. The relevant preheating processes are charged- and neutral-current reactions on nuclei in the iron and also silicon mass range. So far, no detailed collapse simulation including preheating has been performed. The relevant cross sections can be calculated on the basis of shell model calculations for the allowed transitions and RPA studies for the forbidden transitions [48]. The main energy transfer to the matter behind the shock, however, is due to neutrino absorption on free nucleons. The efficiency of this transport depends strongly on the neutrino opacities in hot and very dense neutronrich matter [49]. It is likely also supported by convective motion, requiring multidimensional simulations [51]. Finally, elastic neutrino scattering off nucleons, mainly neutrons, also influences the efficiency of the energy transfer. A non-vanishing strange axialvector formfactor of the nucleon [50] will likely reduce the elastic neutrino-neutron cross section.

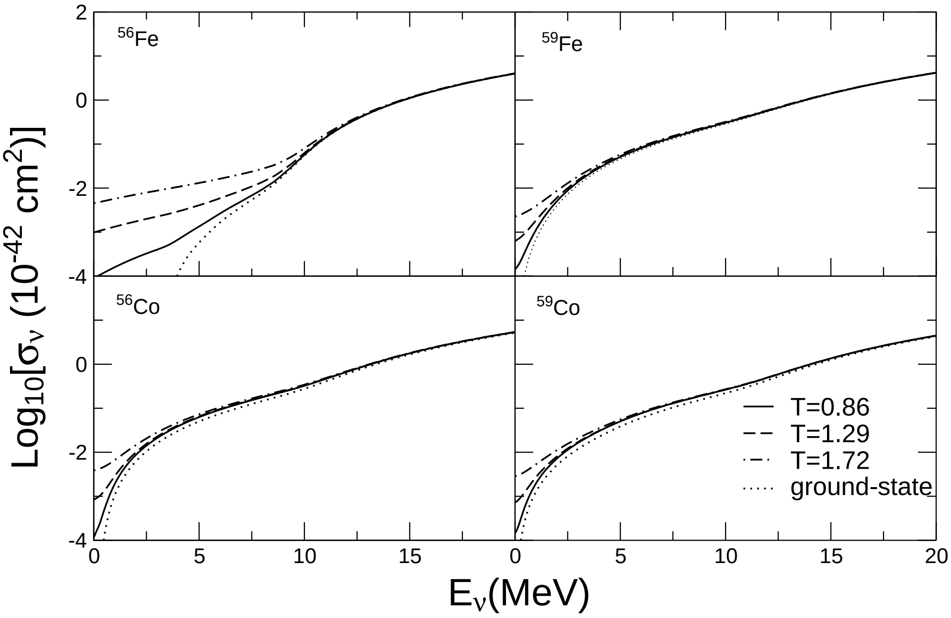

FIG. 5: Cross sections for inelastic neutrino scattering on nuclei at finite temperature. The temperatures are given in MeV (from [47]).

CONCLUSIONS

The recent advances in nuclear many-body modelling has led to noticeable improvements in the nuclear input for core-collapse supernova models. It has been proven that the dynamical timescale of the final collapse is dominated by electron capture on nuclei, and not, as has been the standard picture for many years, by capture on free protons. This has significant consequences for the collapse and changes the Y_e and density profiles throughout the core. However, first supernova simulations do not yield successful explosions.

For the future, other nuclear input needs improvements as well. At first, inelastic neutrino scattering on nuclei should be included in the simulations. Combining modern shell model and RPA codes, the relevant cross sections can be calculated rather reliable, even at finite temperatures, as required for the supernova simulation. The Equation of State plays also an essential role during the collapse, in particular the symmetry energy component and the compression modulus at finite temperatures. Neutrino transport in dense matter requires the consideration of nucleon-nucleon correlations. First attempts into this direction have been taken based on RPA calculations, but more sophisticated approaches are desirable. Besides better nuclear input, improved description of multidimensional effects in supernova models will attract much attention in coming years. This will also include the effects of rotation or magnetic fields on the explosions.

Acknowledgement

The work presented here has benefitted from fruitful discussions and collaborations with Alexander Heger, Raphael Hix, Thomas Janka, Gabriel Martinez-Pinedo, Jorge Sampaio and Stan Woosley.

[1] K. Langanke, F-K. Thielemann and M. Wiescher, Lecture Notes In Physics, to be published
[2] H.A. Bethe, G.E. Brown, J. Applegate and J.M. Lattimer, Nucl. Phys. **A324** (1979) 487
[3] H.A. Bethe, Rev. Mod. Phys. **62** (1990) 801
[4] P.Goldreich and S.V. Weber, Ap.J. **238** (1980) 991
[5] J.R. Wilson, in *Numerical Astrophysics*, ed. by J.M. Centrella, J.M. LeBlanc and R.L. Bowers, (Jones and Bartlett, Boston, 1985) p. 422
[6] A. Burrows, Ann.Rev.Nucl.Sci. **40** (1990) 181.

[7] A. Mezzacappa *et al.*, Phys. Rev. Lett. **86** (2001) 1935
[8] A. Burrows, Ap.J. **334** (1988) 891.
[9] A. Burrows and B.A. Fryxell, Science **258** (1992) 430.
[10] E. Müller and H.-T. Janka, Astron.Astrophys. **317** (1994) 140
[11] S. Reddy, M. Prakash and J.M. Lattimer, Phys.Rev. D **58** (1998) 3009.
[12] A. Burrows and R.F. Sawyer, Phys.Rev. C **58** (1998) 554.
[13] H.Th. Janka and M. Rampp, Astrophys. J. **539** (2000) L33
[14] J.R. Wilson, in *Fermi and Astrophysics*, ed. R. Ruffini, to be published in Nuovo Cimento
[15] R. Buras, M. Rampp, H.-Th. Janka and K. Kifonidis, Phys. Rev. Lett. 90 (2003) 241101
[16] G.M. Fuller, W.A. Fowler and M.J. Newman, ApJS **42** (1980) 447
[17] G.M. Fuller, W.A. Fowler and M.J. Newman, ApJS **48** (1982) 279
[18] G.M. Fuller, W.A. Fowler and M.J. Newman, ApJ **252** (1982) 715
[19] G.M. Fuller, W.A. Fowler and M.J. Newman, ApJ **293** (1985) 1
[20] T. Oda, M. Hino, K. Muto, M. Takahara and K. Sato, At. Data Nucl. Data Tabl. **56** (1994) 231
[21] E. Caurier, K. Langanke, G. Martínez-Pinedo and F. Nowacki, Nucl. Phys. A **653** (1999) 439.
[22] K. Langanke and G. Martínez-Pinedo, Nucl. Phys. **A673** (2000) 481
[23] D. Frekers, Proccedings COMEX1, Nucl.Phys. A, to be published
[24] M.B. Aufderheide, I. Fushiki, S.E. Woosley and D.H. Hartmann, Ap.J.S. **91** (1994) 389
[25] K. Langanke and G. Martínez-Pinedo, At. Data Nucl. Data Tables **79** (2001) 1
[26] A. Heger, K. Langanke, G. Martinez-Pinedo and S.E. Woosley, Phys. Rev. Lett. **86** (2001) 1678
[27] A. Heger, S.E. Woosley, G. Martinez-Pinedo and K. Langanke, Astr. J. **560** (2001) 307
[28] S.E. Woosley and T.A. Weaver, Astrophys. J. Suppl. 101 (1995) 181
[29] S. W. Bruenn, Astrophys. J. Suppl. **58**, 771 (1985); A. Mezzacappa and S. W. Bruenn, Astrophys. J. **405**, 637 (1993); **410**, 740 (1993)
[30] G. M. Fuller, Astrophys. J. **252**, 741 (1982)
[31] J. Cooperstein and J. Wambach, Nucl. Phys. **A420** (1984) 591
[32] K. Langanke, E. Kolbe and D.J. Dean, Phys. Rev. C **63**, 032801 (2001)
[33] W. Nazarewicz, J. Dudek, R. Bengtsson, T. Bengtsson and I. Ragnarsson, Nucl. Phys. **A435** (1985) 397
[34] O. Sorlin *et al.*, Phys. Rev. Lett. **88**, 092501 (2002)
[35] M.C. Vetterli *et al.*, Phys. Rev. C **45**, 997 (1992)
[36] R.L. Helmer *et al.*, Phys. Rev. C **55**, 2802 (1997)
[37] C.W. Johnson, S.E. Koonin, G.H. Lang and W.E. Ormand, Phys. Rev. Lett. **69** (1992) 3157
[38] S.E. Koonin, D.J. Dean and K. Langanke, Phys. Rep. **278** (1997) 1
[39] J. Hubbard, Phys. Lett. **3** (1959) 77; R.D. Stratonovich, Sov. Phys. - Dokl. **2** (1958) 416
[40] W.R. Hix, Ph.D. thesis, Harvard University, 1995.
[41] K. Langanke *et al.*, Phys. Rev. Lett. 90 (2003) 241102
[42] R.W. Hix *et al.*, submitted to Phys. Rev. Lett.
[43] H-Th. Janka *et al*, to be published
[44] W.C. Haxton, Phys. Rev. Lett. **60** (1988) 1999
[45] S.W. Bruenn and W.C. Haxton, Astr. J. **376** (1991) 678
[46] J.M. Sampaio, K. Langanke and G. Martinez-Pinedo, Phys. Lett. **B511** (2001) 11
[47] J.M. Sampaio, K. Langanke, G. Martinez-Pinedo and D.J. Dean, Phys. Lett. **B529** (2002) 19
[48] J. Toivanen *et al.*, Nucl. Phys. **A694** (2001) 395
[49] S. Reddy, M. Prakash, J.M. Lattimer and S.A. Pons, Phys Rev **C59** (1999) 2888
[50] M.J. Musolf *et al.*, Phys. Rep. **239** (1994) 1; J. Ashman *et al.*, Nucl. Phys. **B328** (1989) 1
[51] A. Mezzacappa, Nucl. Phys. **A688** (2001) 158c